Characterization of spatial and temporal variations in the optical properties of tissuelike media with diffuse reflectance imaging

Francesco Fabbri, Maria Angela Franceschini, and Sergio Fantini

We describe a method to characterize spatial or temporal changes in the optical properties of turbid media using diffuse reflectance images acquired under broad-beam illumination conditions. We performed experiments on liquid phantoms whose absorption (μ_a) and reduced scattering (μ_s') coefficients were representative of those of biological tissues in the near infrared. We found that the relative diffuse reflectance R depends on μ_a and μ_s' only through the ratio μ_a/μ_s' and that dependence can be well described with an analytical expression previously reported in the literature [S. L. Jacques, Kluwer Academic Dordrecht (1996)]. We have found that this expression for R deviates from experimental values by no more than 8% for various illumination and detection angles within the range 0°–30°. Therefore, this analytical expression for R holds with good approximation even if the investigated medium presents curved or irregular surfaces. Using this expression, it is possible to translate spatial or temporal changes in the relative diffuse reflectance from a turbid medium into quantitative estimates of the corresponding changes of $(\mu_a/\mu_s')^{1/2}$. In the case of media with optical properties similar to those of tissue in the near infrared, we found that the changes of μ_a/μ_s' should occur over a volume approximately 2 mm deep and 4 mm × 4 mm wide to apply this expression.

OCIS codes: 170.6510, 170.0110, 170.7050.

1. Introduction

Optical imaging of biological tissue with a charge-coupled device (CCD) camera under broad-beam illumination conditions is a powerful tool for investigating superficial tissue layers with high spatial resolution. For instance, this approach has been used to obtain ~50-μm-resolution, *in vivo* images of the cerebral cortex in animal models[1–3] and in humans.[4] The use of infrared light offers advantages over visible light in that it can sample deeper regions of tissue (>500 μm), it better penetrates the dense and thinned skull in brain studies, and it is less sensitive to blood vessel artifacts.[5] Furthermore, the increased optical penetration depth offered by near-infrared (NIR) light lends itself to noninvasive imaging applications such as the *in vivo* imaging of tumors with fluorescent contrast agents.[6–9] These optical imaging approaches rely on spatial and temporal changes in the diffuse reflectance that are associated with brain activity, modifications to the local hemodynamics or metabolic rate or to both and accumulation or activation of a fluorescent probe at a cancerous site, etc. In most cases, these changes in the diffuse reflectance are only analyzed qualitatively. However, it is been recently reported that a quantitative analysis of the mean reflectances of human skin defects can be used to discriminate cutaneous melanoma from other pigmented cutaneous lesions.[10,11] Consequently, to translate the differences of the diffuse reflectance of a biological tissue in differences of the optical properties may further improve the effectiveness of this imaging method, by allowing for a quantitative measurement of the local changes in the concentration of NIR chromophores.

A number of models have been developed to express the diffuse reflectance from a turbid medium (under broad-beam illumination conditions) in terms of the optical properties of the medium.[12–19] We briefly review some of these models in Section 2. All

The authors are with the Department of Biomedical Engineering, Bioengineering Center, Tufts University, 4 Colby Street, Medford, Massachusetts 02155. M. A. Franceschini is also with Massachusetts General Hospital, NMR Center, Thirteenth Street Building 149, Charlestown, Massachusetts 02129. F. Fabbri's e-mail address is francesco.fabbri@tufts.edu.

Received 27 August 2002; revised manuscript received 20 November 2002.

0003-6935/03/163063-10$15.00/0

of these models make several assumptions about the geometry of illumination or collection or both, the angular distribution of the light scattering within the medium, and the flatness of the air–medium boundary, etc. These assumptions are often crude approximations of practical *in vivo* measurements on tissue, and they may have a significant effect on the evaluation of the absolute reflectance (i.e., the ratio of the diffusely reflected light flux to the incident flux) that is usually considered in these models. Because most of the applications of diffuse optical imaging are aimed at measuring spatial or temporal changes in the diffuse reflectance, we focus our attention on the relative diffuse reflectance [i.e., the ratio of the diffuse reflectance at one location (or time) R_2 to that at a different location (or different time) R_1]. We have found that the relative diffuse reflectance is highly insensitive to the geometry of illumination and collection; therefore, it may be robustly measured on tissue *in vivo*. Furthermore, if the ratio R_2/R_1 can be expressed as a function of the difference μ_2-μ_1 [where μ_1 and μ_2 indicate some combination of the optical properties at locations (or times) 1 and 2, respectively], then by inverting this functional dependence one can translate a measurement of R_2/R_1 into the corresponding change in the optical properties of the medium μ_2-μ_1. Inversion of this functional dependence is the general idea behind this research, which is aimed at enhancing the information content of diffuse optical images *in vivo*.

Here is a description of what we have done in this research:

- we analyzed several theoretical models that express the dependence of the diffuse reflectance on μ_a and μ_s' (the reduced scattering coefficient[18]) using different assumptions about the geometric configuration and the light scattering inside the medium;
- we measured the dependence of the diffuse reflectance on the optical coefficients μ_a and μ_s' of a tissuelike medium for a given experimental configuration;
- we measured the sensitivity of that dependence caused by changes in the illumination and detection angles, to get indications of the sensitivity to the curvature of the medium boundary;
- we identified, between the described models that express the relative diffuse reflectance as a function of μ_a and μ_s', an expression for the diffuse reflectance that presents the best agreement with our experimental results;
- we estimated the sample volume that affects the measured diffuse reflectance.

1. Models for Diffuse Reflectance in Turbid Media

There are several theoretical and numeric models that have been used to express the diffuse reflectance from a turbid medium as a function of its optical properties. Every model makes specific assumptions about the illumination and detection geometries and about the optical characteristics of the medium. In this section, we review some of these models, which we use to interpret our results and to get indications on the effects of individual geometric or spatial parameters of the diffuse reflectance.

A. Boltzmann Transport Equation

The Boltzmann transport equation[19] (BTE) describes light propagation in scattering and absorbing media, such as biological tissue. This equation involves three optical properties, namely, the absorption coefficient μ_a, the scattering coefficient μ_s, and the scattering phase function.[18] Under steady-state conditions the BTE can be written as follows[20]:

$$\mathbf{s}\cdot\nabla L(\mathbf{r}, \mathbf{s}) = -(\mu_a + \mu_s) L(\mathrm{r}, \mathrm{s}) + \mu_s \int_{4\pi} \mathrm{p}(\mathbf{s}, \mathbf{s}') L(\mathbf{r}, \mathbf{s}') \mathrm{d}\omega' , \quad (1)$$

where $L(\mathbf{r}, \mathbf{s})$ is the radiance of light at position $\mathbf{r}$ along direction $\mathbf{s}$, μ_a is the absorption coefficient, μ_s is the scattering coefficient, $\mathrm{d}\omega'$ is the element of solid angle in direction $\mathbf{s}'$, and $p(\mathbf{s}, \mathbf{s}')$ is the phase function.[18] Equation (1) holds when one can neglect fluorescence, polarization, and the interactions between photons[21] (such as interference and diffraction effects).

The Boltzmann equation has general applicability and can be used, in particular, to find the diffuse reflectance from a medium illuminated with a broad beam. However, because of the difficulty of solving the equation directly, several approximations have been made. Chandrasekhar[21] first solved the equation, and Giovanelli[14] then elaborated the results to find the diffuse reflectance under the following simplified conditions:

- semi-infinite medium;
- homogeneous medium;
- either perfectly diffuse or collimated and perpendicular irradiance (broad beam);
- isotropic scattering [$p = (1/4\pi)$] or phase function $p = (1 + x \cos\theta)/4\pi$, where θ is the scattering angle, and x is a parameter that assume values in the range 0–1.

The solution is not analytical, and Giovanelli[14] tabulated the values of the total diffuse reflectance for various values of albedo in the cases of refractive-index matching condition and either isotropic scattering or anisotropic scattering corresponding to x of 0, 0.25, 0.5, 0.75, and 1. Giovanelli[14] tabulated a few diffuse reflectance values also in the case of a refractive-index mismatch at the medium surface of 1.33 or 1.5.

B. Approximate Solutions of the Boltzmann Transport Equation

There are numerous theories leading to approximate solutions to the BTE for the diffuse reflectance under orthogonal broad-beam illumination conditions; we consider in particular the 3-flux theory[16,22] and the diffusion theory.[17,12] These two methods lead to

simplified formulas that provide an expression for the diffuse reflectance of a semi-infinite medium. Burger *et al.*[16,22] showed that in the case of isotropic scattering, the results of the 3-flux theory agree well with the results tabulated by Giovanelli[14] for the same configuration. However, the application of the 3-flux theory to biological tissue gives rise to two main problems:

- light scattering in biological tissues is strongly anisotropic, but the 3-flux theory leads to an easy formula for the diffuse reflectance only for the case of isotropic scattering
- biological tissues can have curved and irregular boundaries; thus it is not always possible to achieve a condition of normal incidence of irradiation.

In diffusion theory, the scattering phase function is represented by the mean cosine of the scattering angle g, which is combined with the scattering coefficient to give the reduced scattering coefficient $\mu_s' = \mu_s(1 - g)$. The optical reduced albedo a' is defined as $\mu_s'/(\mu_a + \mu_s')$. Using diffusion theory, Flock *et al.*[17] found an equation that expresses the diffuse reflectance R of a semi-infinite medium under orthogonal broad-beam illumination as a function of the optical reduced albedo a':

$$R_\infty = \frac{a'}{1 + 2k(1 - a') + (1 + 2k/3)[3(1 - a')]^{1/2}}, \tag{2}$$

where $k = (1 - r_d)/(1 + r_d)$ and r_d is the internal reflection coefficient of the medium. Equation (2) can be employed to obtain the diffuse reflectance from a medium when the optical reduced albedo and the internal reflection coefficient are known. Equation (2) is applicable if the detected photons have traveled diffusively within the medium, which requires that they have undergone many scattering events. Therefore, Eq. (2) may not be accurate in a case in which a large part of the detected signal comes from very superficial medium layers, where the detected photons may have undergone just a few scattering events.

C. Kubelka–Munk theory

Assuming all the hypotheses of Chandrasekhar–Giovanelli, but considering only the case of isotropic scattering, matched boundaries, and diffuse irradiation at the sample, Kubelka and Munk developed a 2-flux approximation method[17,21,23] that led to the following equation for the diffuse reflectance (R_∞):

$$R_\infty = 1 + \frac{K}{S} - \left(\frac{K^2}{S^2} + 2\frac{K}{S}\right)^{1/2}, \tag{3}$$

where K and S are the Kubelka–Munk's absorption and scattering coefficients, respectively, which do not coincide with μ_a and μ_s. Several researchers[24–29] tried to find relations between the two sets of coefficients. Mudgett and Richards[29] obtained an approximated equation that relates the ratios K/S and μ_a/μ_s to the first two coefficients of the series of Legendre that expresses the phase function. This formula, obtained in the case of a perfectly diffuse irradiation, reduces to the following expression for isotropic scattering:

$$\frac{\mu_a}{\mu_s} \approx \frac{3K}{8S}. \tag{4}$$

The same result was obtained by comparison of the Kubelka–Munk's formula with the Chandrasekhar's exact solution.[24] Equation (4) holds also for an anisotropic phase function that is symmetric with respect to $\theta = \pi/2$.[29,30] However, in the case of a phase function that shows forward and backward peaks of different magnitudes (which is the case for almost all biological tissues) the use of the Kubelka–Munk's theory may lead to errors. Furthermore, the Kubelka–Munk theory is strictly applicable only in the case of perfectly diffuse irradiation. Nevertheless, Burger *et al.*[16,22] showed that it is possible to generalize the Kubelka–Munk theory for a configuration that uses perpendicular illumination, provided that the ratio between μ_a/μ_s and K/S is set to 0.27 instead of 3/8 (or 0.375) as in Eq. (4). We point out that the value 0.27 is obtained empirically. Furthermore, the Kubelka–Munk requirement of a diffuse illumination is impractical for some reflectance measurements. The case of normal incident irradiation can be treated with the 3-flux theory, which provides the advantage that the scattering and the absorbing coefficients in the formula are the same as in Mie theory.

D. Adding-Doubling Method

Recently, Prahl *et al.*[31] introduced a new method to measure the optical properties of turbid materials by iterating an adding-doubling solution of the radiative transport equation. By using the adding-doubling method, Prahl et al.[31] found values of the total reflection by considering normal incident irradiation and different values for albedos, optical thickness, matched and unmatched boundary conditions, and isotropic and anisotropic scattering.[32] They compared the values obtained in the case of isotropic scattering with the tabulated values of Giovanelli,[14] finding them in good agreement. It is interesting to point out that, in the anisotropic case, Prahl *et al.*[19] employ the Henyey–Greenstein phase function that is often used to describe light scattering in biological tissue.[33]

More recently, using both adding-doubling and Monte Carlo methods, Jacques[34] obtained the following analytical expression for the diffuse reflectance from a semi-infinite medium that presents anisotropic scattering as described by the Henyey–Greenstein phase function and considering a

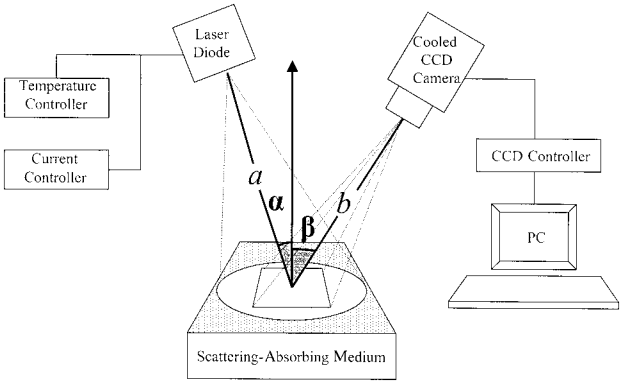

Fig. 1. Experimental setup for the acquisition of relative diffuse reflectance images of turbid media. CCD, charge-coupled device; PC, personal computer.

refractive-index mismatch of 1.33 between medium and air[32]:

$$R_\infty = \exp\left\{\frac{-7.8}{\left[3\left(1+\frac{\mu_s'}{\mu_a}\right)\right]^{1/2}}\right\}. \quad (5)$$

Jacques[35] uses this formula to express the diffuse reflectance of the human skin illuminated by collimated perpendicular radiation. In a successive publication, he established that the value of 7.8 in Eq. (5) is neither a constant nor just a function of the refractive-index mismatch but that it depends on the ratio between μ_a and μ_s'.[34] However, Eq. (5) represents an important step toward the quest for an analytical expression for the diffuse reflectance that takes into account the strong anisotropy of light scattering inside biological tissues.

2. Materials and Methods

A. Optical Imaging Setup

Figure 1 shows a schematic diagram of the experimental setup. We used a laser diode (Sharp LT025MD) that emits a divergent beam with elliptical cross section. The beam divergences along the major and minor axes of the ellipse are approximately 26° and 10°, respectively. When the laser is at a distance a of 30 cm from the sample (typical distance used in our measurements), the illuminated area is an ellipse with axes of approximately 14 and 5 cm, respectively. We used an LDX-3525 (ILX-Lightwave, Bozeman, Montana) precision current source to supply the laser with a current of 120 mA, resulting in a constant output power of approximately 40 mW. The temperature of the laser was stabilized at 25 °C with an LDT-5525 (ILX-Lightwave, Bozeman, Montana) thermoelectric temperature controller, so that the emitted wavelength was fixed at 784 nm (from the datasheet of the laser). This wavelength choice falls within the diagnostic optical window for biological tissue, where the tissue absorption is minimized,[36,37] so that the optical penetration depth of the radiation in the medium is maximized. The spatially resolved optical detection was performed with a CCD camera (Vers Array 512B, Roper Scientific, Trenton, New Jersey). The CCD lens was a 24 mm f2.8 wide angle (Vivitar, Newbury Park, California). This choice provides a relatively large solid angle of light collection that results in a 14 cm × 14 cm imaged area at the minimum working distance b of 30 cm, so that the linear dimension of the pixel corresponds to 0.27 mm.

B. Tissuelike Sample

We used a liquid phantom consisting of Liposyn-10%, water, and black India ink inside a container of dimensions 12 cm × 10 cm × 4 cm (length, width, depth). Liposyn is a brand name for an intravenous nutrient that contains lipids and that is similar in composition to other brands like Intralipid and Nutralipid (100 ml of Liposyn-10% contain 5 g of soybean oil, 5 g of safflower oil, and 2.5 g of glycerin in water). Lipid suspensions such as these are often used in the biomedical optics field for simulating biological tissue[38,40] because they show strong forward scattering and weak absorption at visible and NIR wavelengths, similar to biological tissues. A diluted solution of India ink[38,41] provides an appropriate absorber. We made the phantom by mixing two calibrated solutions in deionized water: the first one of Liposyn-10% and the second one of India ink to modify, respectively, the reduced scattering coefficient and the absorption coefficient. We varied the relative concentrations of these two solutions by controlled steps, so that the optical coefficients of the phantom at 784 nm were in the ranges $0.03\ \text{cm}^{-1} < \mu_a < 0.5\ \text{cm}^{-1}$ with constant $\mu_s' = 8.6 \pm 0.4\ \text{cm}^{-1}$ and $1\ \text{cm}^{-1} < \mu_s' < 20\ \text{cm}^{-1}$ with constant $\mu_a = 0.056 \pm 0.003\ \text{cm}^{-1}$. These values are representative of the absorption and reduced scattering coefficients of biological tissue at NIR wavelengths.[42] The optical properties of the two solutions were calibrated by use of a multidistance frequency-domain method.[43] The measured value of μ_s' at 784 nm of the 10% concentrated solution of Liposyn-10% was $9.6 \pm 0.5\ \text{cm}^{-1}$, whereas the measured value of μ_a for the India ink solution was $0.18 \pm 0.01\ \text{cm}^{-1}$. As reported in the literature,[43] our measurements confirmed that, in the ranges considered, the absorption coefficient is determined by the ink concentration, whereas the scattering coefficient is determined by the Liposyn concentration. When we varied the Liposyn and ink concentrations, we took care to keep the volume of the liquid sample (and thus the level of the liquid in the dish) constant. Throughout the measurement session, we stirred the aqueous suspension before every image acquisition to ensure uniformity and to prevent the settlement of the lipids. We verified that the medium can be considered as semi-infinite, because the light that reached the boundaries of the dish had no effect on the measured reflectance.

C. Measurements of Diffuse Reflectance

Figure 1 defines the illumination distance (a), the angle of incidence (α), the collection distance (b),

and the angle (β). Initially, the laser was placed with its illumination axis perpendicular to the surface of the liquid ($\alpha = 0°$) at a distance $a = 30$ cm from the sample. The CCD camera was at a distance $b = 30$ cm and at an angle $\beta = 15°$. In this configuration, we acquired images of the diffuse reflectance of the medium for different values of its optical properties. First, we kept the reduced scattering coefficient of the medium at a value of 8.6 ± 0.4 cm^{-1}, and we varied the absorption coefficient over the range 0.03–0.5 cm^{-1}. Then, we kept the absorption coefficient fixed at a value of 0.056 ± 0.003 cm^{-1}, and we varied the reduced scattering coefficient over the range 1–20 cm^{-1}. The acquired images were elaborated as follows:

- We considered a relatively large imaged area (9 cm × 4 cm), composed of pixels that were at least 2 cm away from the edge of the container;
- We performed a dark-current correction[44] consisting of subtracting from each image an image acquired with the same integration time but at closed shutter;
- We performed a flat-field correction[44] by dividing each image by the image measured on a reference medium containing only scattering particles (Liposyn) and no ink. Such a reference medium had $\mu_a = 0.024 \pm 0.001$ cm^{-1} and $\mu_s' = 8.6 \pm 0.4$ cm^{-1}. This procedure corrects for the inhomogeneity of illumination. As a result, the measurements of diffuse reflectance are relative to the reference medium. We took the average reading over all pixels to increase the signal-to-noise ratio.

We performed a test to measure the effect that the geometric parameters of illumination and detection have on the dependence of the diffuse reflectance on the medium optical parameters. This test consisted of repeating five times the reflectance measurements, described above, for different values of the angle of illumination (α) and collection (β).

To define the volume of the medium that affects the detected signal at a given pixel, we scanned a strongly absorbing target inside the medium using a micrometric translator. In this fashion we determined the depth and lateral size of the sample volume that affects the diffuse reflectance at a specific pixel. We performed this test on a medium with $\mu_a = 0.050 \pm 0.003$ cm^{-1} and $\mu_s' = 8.6 \pm 0.4$ cm^{-1} values that are representative of biological tissue in the NIR. The totally absorbing target was a small cylinder with a base diameter of 0.75 mm and a height of 10 mm. Using a geometric configuration with $\alpha = 15°$, $\beta = 0°$, $a = 30$ cm, and $b = 30$ cm, we acquired diffuse reflectance images of the medium, varying the target immersion depth from 0 to 4 mm by increments of 1 mm. The image of the medium without the absorbing target was used for flat-field correction.

3. Results

Figure 2 shows the dependence of the relative diffuse reflectance on the ratio between the absorption and the reduced scattering coefficients of the medium. Closed circles refer to data taken on media with a fixed reduced scattering coefficient and variable absorption, whereas the open squares refer to data taken on media with a fixed absorption and variable scattering. The 5% relative error in the measurements of μ_a and μ_s' of the original scattering and absorbing solutions results in a systematic error (shown by the error bars in Fig. 2) for each of the two curves. The two data sets coincide to within such errors, indicating that the diffuse reflectance depends only on the ratio between the two optical coefficients.

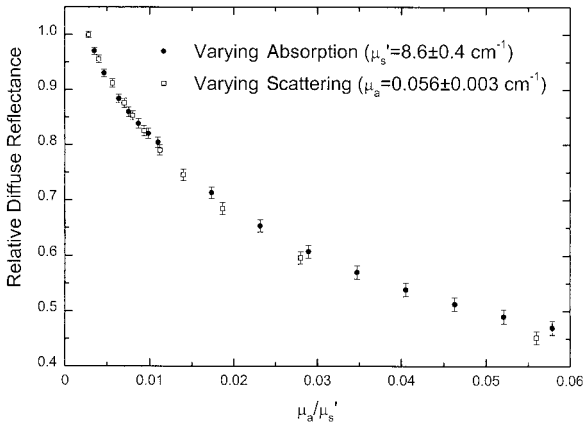

Fig. 2. Experimental data of relative diffuse reflectance as a function of the ratio of the absorption and reduced scattering coefficients. We obtained the two data sets by varying the absorption coefficient at constant $\mu_s' = 8.6 \pm 0.4$ cm^{-1} (closed circles) and by varying the reduced scattering coefficient at constant $\mu_a = 0.056 \pm 0.003$ cm^{-1} (open squares), respectively.

When we repeated these measurements using different values of angle of illumination ($\alpha = 0°$, $\alpha = 15°$, $\alpha = 30°$), angle of collection ($\beta = 0°$ and $\beta = 15°$), and distance between CCD camera and sample ($b = 30$ cm and $b = 40$ cm), we found similar results. Table 1 reports the measured data for the various cases and the maximum difference in the relative reflectance caused by changing the experimental geometry. The maximum deviation is 8%.

Figure 3 shows the effect of the cylindrical absorbing target on the diffuse reflectance for depths of immersion in the medium of 0, 1, 2, and 3 mm (we do not show in Fig. 3 the case for depth of 4 mm). The medium had $\mu_a = 0.050 \pm 0.003$ cm^{-1} and $\mu_s' = 8.6 \pm 0.4$ cm^{-1}. The curves in Fig. 3 represent the diffuse reflectance measured along a line that contains the projection of the absorbing target on the sample surface. In each image, all lines containing the projection of the target had the same shape within experimental errors. When the target is 2 mm deep in the medium it becomes clearly detectable since the peak in the diffuse reflectance is lower than all of the values at the other pixels. Figure 3 also shows that when the target is on the surface (i.e., depth = 0), it affects the intensity profile of the diffuse reflectance image laterally for a distance of approximately 2 mm.

Table 1. Relative Diffuse Reflectance for 11 Values of μ_a/μ_s' and for Various Geometric Parameters (α, β, and b)[a]

μ_a/μ_s'	Relative Diffuse Reflectance					Δ Max (%)
0.0035	1	1	1	1	1	0
0.0077	0.86	0.86	0.87	0.87	0.86	1
0.012	0.76	0.78	0.79	0.78	0.78	4
0.016	0.70	0.72	0.73	0.72	0.72	4
0.02	0.65	0.67	0.68	0.67	0.67	4
0.025	0.61	0.63	0.64	0.63	0.62	5
0.029	0.57	0.60	0.61	0.59	0.59	7
0.033	0.54	0.57	0.58	0.56	0.55	7
0.037	0.52	0.54	0.56	0.54	0.53	7
0.041	0.50	0.52	0.53	0.52	0.50	6
0.046	0.48	0.50	0.52	0.50	0.48	8
α(°)	15	15	0	0	30	
β(°)	0	15	15	15	0	
b(cm)	30	30	30	40	30	

[a]Parameters are defined in Fig. 1. In the last column, we give the maximum discrepancy caused by changing the experimental geometry.

4. Discussion

The measurements performed with our experimental setup show that the diffuse reflectance of a semi-infinite turbid medium depends on μ_a and μ_s' only through their ratio. This result has been reported by previous theoretical[14,15,17] and experimental[45] studies in the particular cases of isotropic scattering and either diffuse or collimated irradiation. In some cases, it has been reported that the laws valid for the isotropic scattering also apply to anisotropic scattering, provided that the scattering coefficient is replaced with the reduced scattering coefficient.[21,46,47] However, Fig. 4 shows that some theoretical models predict a dependence of the diffuse reflectance on μ_a/μ_s' that is different from the one found in our measurements. We observed deviations of 33% by comparing our relative diffuse reflectance measurements with the Kubelka–Munk curve [Eq. (3)] that is a good fit [using the Mudgett's and Richard's assumptions in Eq. (4)] of the data tabulated by Giovanelli[14] in the case of diffuse irradiation (after replacing μ_s with μ_s'). On the other hand, we found deviations of 27% by comparing our measurements with the reflectance values obtained by fitting the data tabulated by Giovanelli[14] in the case of collimated perpendicular irradiation (after replacing μ_s with μ_s' and using the fit curve introduced by Burger *et al.*[16,22]). All curves of diffuse reflectance reported in Fig. 4 are normalized to 1 when $\mu_a/\mu_s' = 0.00347$.

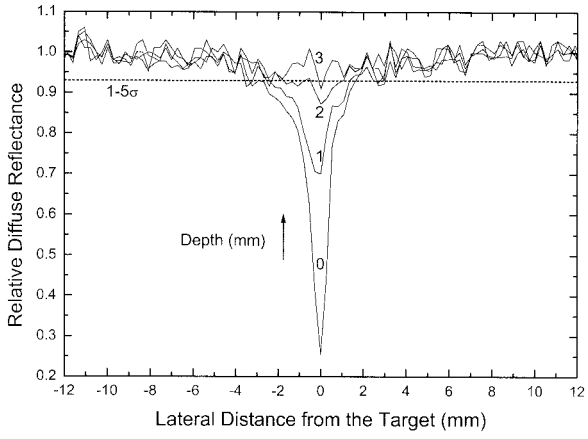

Fig. 3. Profiles of diffuse reflectance intensity for four different values of immersion depth of the small, totally absorbing inhomogeneity. The medium had optical properties of $\mu_a = 0.050 \pm 0.003$ cm^{-1} and $\mu_s' = 8.6 \pm 0.4$ cm^{-1}. The curves are normalized to the intensity collected far away from the inhomogeneity. The horizontal line represents the value that is 5 standard deviations (σ) below the average intensity of 1 measured away from the inhomogeneity.

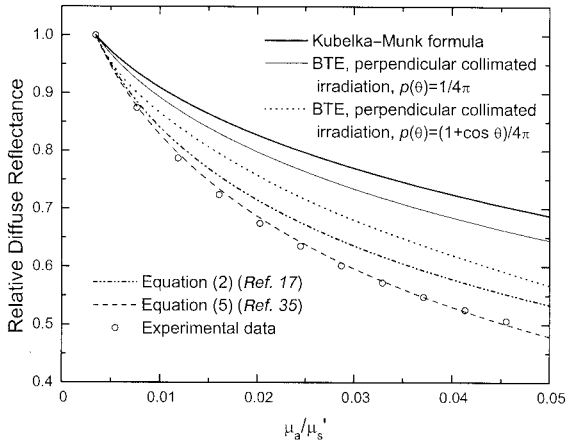

Fig. 4. Comparison between our experimental data (open circles) of relative diffuse reflectance versus μ_a/μ_s' and several theoretical models: Kubelka–Munk [Eq. (3)], valid for diffuse irradiation, matched refractive index, and isotropic scattering (dark solid curve); BTE for orthogonal collimated irradiation, matched refractive index, and isotropic scattering[14] (light solid curve); BTE with anisotropic scattering described by a phase function $p = (1 + \cos\theta)/4\pi$[14] (dotted curve); diffusion theory [Eq. (2)] for a refractive-index mismatch of 1.33 (dash-dotted curve); and adding-doubling and Monte Carlo methods [Eq. (5)] for the Henyey–Greenstein phase function and refractive-index mismatch of 1.33 (dashed curve). In the graph, all the theoretical curves are normalized to 1 for $\mu_a/\mu_s' = 0.00347$.

From our measurements it appears that the geometry of illumination and detection is not likely to affect the dependence of the relative reflectance on μ_a/μ_s' significantly. In fact, Table 1 shows that the diffuse reflectance for different geometric parameters varies at most by 8%. Furthermore, in the case of $\alpha = 0°$ (i.e., the laser axis perpendicular to the medium surface), we also considered a small central portion (1 cm × 1 cm) of the medium. The reflectance signal from this target has contributions mainly from its illumination and from the illumination of its close surroundings; in this portion of the medium the illumination was almost normal to the medium surface. Also for this case, we found exactly the same deviations of the diffuse reflectance from the theoretical models. The data, tabulated by Giovanelli[14] for the case of refractive-index mismatch between air and medium, are not enough for a meaningful comparison with our experimental results over the μ_a/μ_s' range that we considered. The comparison with the data of Giovanelli[14] is therefore performed with the case of same refractive index between air and medium, which may account, at least in part, for the deviations between the experimental results and the theoretical data of Giovanelli.[14] However, the deviations are likely caused also by the anisotropic scattering in the medium used in our experiments. Giovanelli[14] demonstrated the sensitivity of the diffuse reflectance to the scattering anisotropy when he considered the diffuse reflectance for isotropic scattering and for a linearly anisotropic phase function. Figure 4 shows also the curves resulting from fitting the data tabulated by Giovanelli[14] in these two cases, indicating the different dependence of the relative diffuse reflectance on μ_a/μ_s' in the isotropic and the anisotropic scattering cases. Furthermore, Reichman[48] developed a refined version of the 2-flux model, assuming collimated incident radiation to find a law that expresses the diffuse reflectance as a function of the optical parameters. His theory shows very good agreement with the more exact solution of the equation of radiative transfer,[20] except for the case of highly anisotropic scattering. In Subsection 1.B, we mentioned that one can use diffusion theory to express the dependence of the diffuse reflectance on the optical properties μ_a and μ_s' of a turbid medium under matched or unmatched boundary conditions. This dependence is given by Eq. (2).[17] By comparing our experimental data with Eq. (2), we found a maximum discrepancy of 10% as shown in Fig. 4 (considering a refractive-index mismatch of 1.33 between medium and air). We found that in our measurements the signal comes from a shallow superficial layer of the medium, so that a large number of detected photons may not have reached a diffusive regime of propagation within the medium. This fact may account for the discrepancy between our experimental data and the diffusion theory expression of the reflectance [Eq. (2)]. We noted previously that Jacques[34,35] expressed the absolute diffuse reflectance of a semi-infinite medium as reported in Eq. (5). Our relative diffuse reflectance measurements were well described by our introducing an arbitrary normalization factor K into Eq. (5):

$$R = K \exp\{-7.8/[3(1 + \mu_s'/\mu_a)]^{1/2}\}. \quad (6)$$

Figure 4 shows the good agreement between our experimental data set of diffuse reflectance and the expression in Eq. (6), within maximum deviations of 2%. The ratio of the relative diffuse reflectance values R_1 and R_2 at two locations (for spatial changes) or at two times (for temporal changes) cancels out the unknown factor K in Eq. (6), and one can find the corresponding change in the $(\mu_a/\mu_s')^{1/2}$ of the investigated medium. In fact, using Eq. (6) and considering that $\mu_s'/\mu_a \gg 1$ (a condition commonly verified for biological tissue), we found after some algebra

$$-A \ln(R_2/R_1) = (\mu_a/\mu_s')_2^{1/2} - (\mu_a/\mu_s')_1^{1/2} = \Delta[(\mu_a/\mu_s')^{1/2}], \quad (7)$$

where $A = 3^{1/2}/7.8 \sim 0.22$ and the subscripts 1 and 2 indicate the different locations or the different times.

The measurement of the variation in $(\mu_a/\mu_s')^{1/2}$ may be useful for diagnostic applications *in vivo*. In fact, in many cases the presence of biological tissue inhomogeneities, such as tumors, fluid-filled cysts, ischemic regions, hemorrhages, and skin defects, are often associated with variations in the optical properties, which result in local changes in the ratio μ_a/μ_s'.[10,11] In some cases, a temporal change in the ratio μ_a/μ_s' may be induced by the administration of extrinsic dyes. We propose to use Eq. (7) for measurements of variations in the optical parameters of biological tissue. Moreover, Jacques obtained Eq. (5) using the Henyey–Greenstein function for the scattering phase function, which is often used for simulating anisotropic scattering in biological tissue. Furthermore, we found that Eq. (6), derived from Eq. (5), well expresses the experimental data of diffuse reflectance on a sample that had optical properties similar to those of biological tissue in the NIR.

As an example of application, we illustrate how the relative diffuse reflectance measurements can be employed to measure the difference in the absorption coefficient between two locations where the scattering properties are unchanged. For example, it has been reported that several kinds of tumors have μ_s' similar to the rest of the tissue, whereas μ_a may be much higher.[49–52] In this case, the two relative diffuse reflectance values R_1 and R_2 (inside and outside the tumor) can be used to obtain $\Delta\mu_a$, namely, the difference between the absorption coefficients inside and outside the tumor. In fact, in the case $\mu_{s'1} = \mu_{s'2} = \mu_s'$, Eq. (7) can be used to express $\Delta\mu_a$ as follows:

$$\Delta\mu_a = (A\mu_s')^{1/2}\ln\left(\frac{R_1}{R_2}\right)\left[(A\mu_s')^{1/2}\ln\left(\frac{R_1}{R_2}\right) + 2(\mu_{a1})^{1/2}\right]. \quad (8)$$

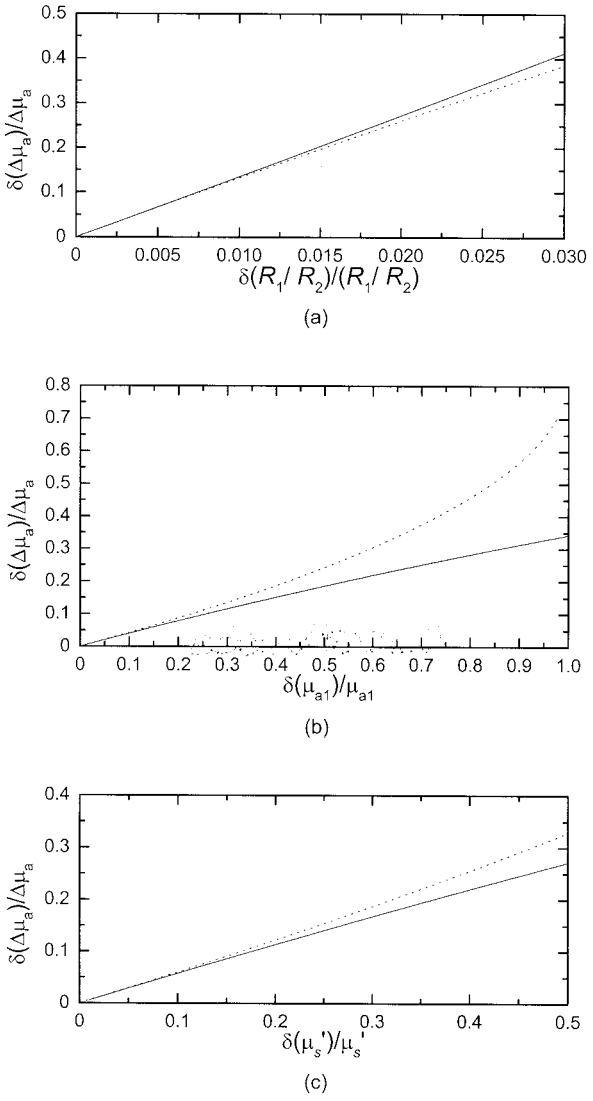

Fig. 5. Errors in the determination of $\Delta\mu_a$ by use of Eq. (8) caused by overestimates (solid lines) or underestimates (dashed lines) (δ) of R_1/R_2, μ_{a1}, and μ_s'. The graphs (a), (b), and (c), show the relative errors in $\Delta\mu_a$ versus the relative errors in R_1/R_2, μ_{a1}, and μ_s', respectively.

Therefore, this method requires one to know the μ_s' and μ_{a1} of tissue. It is possible to use an estimate of μ_s' and μ_{a1} by measuring them[54] or by using values reported in literature.[43] As reported in Fig. 5, for a medium representative of biological tissue with $\mu_a = 0.1\ \text{cm}^{-1}$ and $\mu_s' = 10\ \text{cm}^{-1}$, even a relative error of 50% in the estimate of μ_a causes a relative error of less than 20% in $\Delta\mu_a$, whereas a relative error of 30% in the estimate of μ_s' can cause a relative error as large as 15% in $\Delta\mu_a$. Therefore, Eq. (8) yields a relatively accurate value of $\Delta\mu_a$, even with rough estimates of μ_s' and μ_a. On the other hand, Fig. 5 shows that this method requires an accurate measurement of R_1/R_2, because a relative error of 2% in R_1/R_2 can cause a relative error as large as 30% in $\Delta\mu_a$. In the measurement on tissuelike media, we estimated a relative error on R_1/R_2 of less than 1%.

We found that a small, totally absorbing target affects the diffuse reflectance over a lateral distance of ~4 mm and a depth of ~2 mm. These results pertain to a medium with absorption and reduced scattering coefficients of $0.050 \pm 0.003\ \text{cm}^{-1}$ and $8.6 \pm 0.4\ \text{cm}^{-1}$, respectively. Therefore, the described method for quantitative estimates of the changes in $(\mu_a/\mu_s')^{1/2}$ from the ratio between the diffuse reflectances R_1/R_2 can be applied if the tissue volume involved has linear dimensions and thicknesses of approximately 4 and 2 mm, respectively.

5. Conclusion

We have presented a method for quantitatively measuring spatial or temporal changes in the optical properties of turbid media from diffuse reflectance images. In our experimental setup, the laser-diode source gives a broad-beam illumination over an extended portion of the investigated medium while a CCD camera detector enables noncontact measurements of diffuse reflectance. Changes in the diffuse reflectance R can be translated, for example, into changes in the absorption coefficient (assuming that the reduced scattering coefficient does not change) by generalization of an analytical expression for the R versus μ_a/μ_s' previously reported by Jacques.[35] This generalized expression has been validated experimentally over a wide range of optical properties ($0.03\ \text{cm}^{-1} < \mu_a < 0.5\ \text{cm}^{-1}$ with μ_s' fixed at $8.6 \pm 0.4\ \text{cm}^{-1}$ and $1\ \text{cm}^{-1} < \mu_s' < 20\ \text{cm}^{-1}$ with μ_a fixed at $0.056 \pm 0.003\ \text{cm}^{-1}$), for illumination angles of 0°, 15°, and 30°, and for collection angles of 0° and 15°. In these ranges, we found a maximum variation of 8% in the dependence of R on μ_a/μ_s'.

Our finding that R depends on μ_a and μ_s' only through the ratio μ_a/μ_s' for the range of experimental conditions considered extends the results of previous theoretical studies[14,15,17] restricted to the cases of isotropic scattering and either diffused or collimated irradiations. The relaxation of the geometric requirements is critical in view of the application of our method to samples with curved or irregular boundaries. While the absolute reflectance is strongly affected by boundary effects, boundary shape, and incidence or collection angles or both, the dependence of the relative reflectance on the ratio μ_a/μ_s' is relatively insensitive to these geometric factors, at least if the medium surface does not present strong irregularities or roughness. In this research, we have found that the ratio between the reflectances at different locations or different times is a function of the difference between $(\mu_{a2}/\mu_s'_2)^{1/2} - (\mu_{a1}/\mu_s'_1)^{1/2}$ (where the subscripts 1 and 2 indicate the two different locations or times). Under particular conditions (for instance $\mu_s'_1 = \mu_s'_2$), it is possible to express the absorption changes ($\Delta\mu_a$) in terms of the measurement ratio R_1/R_2.

We thank Douglas Mayson for his help in the preliminary stages of this research and Angelo Sassaroli for useful discussions. This research was supported by the U.S. National Institutes of Health grant MH-

62854 and by the National Science Foundation grant BES-0093840.

References

1. A. Grinvald, E. Lieke, R. Frostig, C. D. Gilbert, and T. N. Wiesel, "Functional architecture of cortex revealed by optical imaging of intrinsic signals," Nature **324,** 361–364 (1986).
2. D. Y. Ts'o, R. D. Frostig, E. Lieke, and A. Grinvald, "Functional organization of primate visual cortex revealed by high resolution optical imaging," Science **249,** 417–420 (1990).
3. D. M. Rector, R. F. Rogers, J. S. Schwaber, R. M. Harper, and J. S. George, "Scattered-light imaging *in vivo* tracks fast and slow processes of neurophysiological activation," Neouroimage **14,** 977–994 (2001).
4. M. M. Haglund, G. A. Ojeman, and D. W. Hochman, "Optical imaging of epileptiform and functional activity in human cerebral cortex," Nature **358,** 668–671 (1992).
5. R. D. Frostig, "What does *in vivo* optical imaging tell us about the primary visual cortex in primates?" in *Cerebral Cortex*, A. Peters and K. S. Rockland eds. (Plenum, New York, 1994), Vol. 10, pp. 331–358.
6. R. Weissleder, C. H. Tung, U. Mahmood, and A. Bogdanov Jr., "*In vivo* imaging of tumors with protease-activated near infrared fluorescent probes," Nat. Biotechnol. **17,** 375–378 (1999).
7. J. E. Bugaj, S. Achilefu, R. B. Dorshow, and R. Rajagopalan, "Novel fluorescent contrast agents for optical imaging of *in vivo* tumors based on a receptor-targeted dye-peptide conjugate platform," J. Biomed. Opt. **6,** 122–133 (2001).
8. M. Gurfinkel, A. B. Thompson, W. Ralston, T. L. Troy, A. L. Moore, T. A. Moore, J. D. Gust, D. Tatman, J. S. Reynolds, B. Muggenberg, K. Nikula, R. Pandey, R. Mayer, D. J. Hawrysz, and E. M. Sevick-Muraca, "Pharmacokinetics of ICG and HPPH-car for the detection of normal and tumor tissue using fluorescence, near-infrared reflectance imaging: a case study," Photochem. Photobiol. **72,** 94–102 (2000).
9. J. S. Reynolds, T. L. Troy, R. H. Mayer, A. B. Thompson, D. J. Waters, K. K. Cornell, P. W. Snyder, and E. M. Sevick-Muraca, "Imaging of spontaneous canine mammary tumors using fluorescent contrast agents," Photochem. Photobiol. **70,** 87–94 (1999).
10. R. Marchesini, S. Tomatis, C. Bartoli, A. Bono, C. Clemente, C. Cupeta, I. Del Prato, E. Pignoli, A. E. Sichirollo, and N. Cascinelli, "*In vivo* spectrophotometric evaluation of neoplastic and non-neoplastic skin pigmented lesions. III. CCD camera-based reflectance imaging," Photochem. Photobiol. **62,** 151–154 (1995).
11. B. Farina, C. Bartoli, A. Bono, A. Colombo, M. Lualdi, G. Tragni, and R. Marchesini, "spectral imaging approach in the diagnosis of cutaneous melanoma: potentiality and limits," Phys. Med. Biol. **45,** 1243–1254 (2000).
12. L. O. Svaasand, L. T. Norvang, E. J. Fiskertrand, E. K. S. Stopps, M. W. Berns, and J. S. Nelson, "Tissue parameters determining the visual appearance of normal skin and portwine strains," Lasers Med. Sci. **65,** 55–65 (1994).
13. L. O. Svaasand, T. Spott, J. B. Fishkin, T. Pham, B. J. Tromberg, and M. W. Berns, "ctance measurements of layered media with photon-density waves: a potential tool for evaluating deep burns and subcutaneous lesions," Phys. Med. Biol. **44,** 801–813 (1999).
14. R. G. Giovanelli, "Reflection by semi-infinite diffusers," Opt. Acta **2,** 153–162 (1955).
15. A. Schuster, "Radiation through a foggy atmosphere," Astrophys. J. **21,** 1–22 (1905).
16. T. Burger, J. Kuhn, R. Caps, and J. Fricke, "Quantitative determination of the scattering and absorption coefficients from diffuse reflectance and transmittance measurements applied to pharmaceutical powders," Appl. Spectrosc. **51,** 309–317 (1997).
17. S. T. Flock, M. S. Patterson, B. C. Wilson, and D. R. Wyman, "Monte Carlo modeling of light propagation in highly scattering tissues—I: model predictions and comparison with diffusion theory," IEEE Trans. Biomed. Eng. **36,** 1162–1168 (1989).
18. A. J. Welch, M. J. C. van Gemert, W. M. Star, and B. C. Wilson, "Overview of tissue optics," in *Optical Thermal Response of Laser Irradiated Tissue*, A. J. Welch and M. J. C. van Gemert, eds. (Plenum, New York, 1995), Chap. 2.
19. J. J. Duderstadt and L. J. Hamilton, *Nuclear Reactor Analysis* (Wiley, New York, 1976).
20. A. Ishimaru, *Wave Propagation and Scattering in Random Media* (Academic, New York, 1978).
21. S. Chandrasekhar, *Radiative Transfer* (Dover, New York, 1960).
22. T. Burger, H. J. Ploss, J. Kuhn, S. Ebel, and J. Fricke, "Diffuse reflectance and transmittance spectroscopy for the quantitative determination of scattering and absorption coefficients in quantitative powder analysis," Appl. Spectrosc. **51,** 1323–1329 (1997).
23. W. R. Blevin and W. J. Brown, "Total reflectance of opaque diffusers," J. Opt. Soc. Am. **52,** 1250–1255 (1962).
24. G. Kortüm, *Reflectance Spectroscopy: Principles, Methods, Applications* (Springer-Verlag, New York 1969).
25. B. J. Brinkworth, "On the theory of reflection by scattering and absorbing media," J. Appl. Phys. Phys. D **4,** 1105–1106 (1971).
26. B. J. Brinkworth, "Interpretation of the Kubelka-Munk coefficients in reflection theory," Appl. Opt. **11,** 1434–1435 (1972).
27. L. F. Gate, "Comparison of the photon diffusion model and Kubelka-Munk equation with the exact solution of the radiative transport equation," Appl. Opt. **13,** 236–238 (1974).
28. K. Klier, "Absorption and scattering in turbid media," J. Opt. Soc. Am. **62,** 882–885 (1972).
29. P. S. Mudgett and L. W. Richards, "Multiple scattering calculations for technology," Appl. Opt. **10,** 1485–1502 (1971).
30. W. F. Cheong, S. A. Prahl, and A. J. Welch "A review of the optical properties of biological tissues," IEEE J. Quantum Electron. **26,** 2166–2185 (1990).
31. S. A. Prahl, M. J. C. van Gemert, and A. J. Welch, "Determining the optical properties of turbid media by using the adding-doubling method," Appl. Opt. **32,** 559–568 (1993).
32. S. A. Prahl, "Light transport in tissue," Ph.D. dissertation (University of Texas at Austin, Austin, Tex., 1988).
33. S. L. Jacques, C. A. Alter, and S. A. Prahl, "Angular dependence of HeNe laser light scattering by human dermis," Lasers Life Sci. **1,** 309–333 (1987).
34. S. L. Jacques, "Diffuse reflectance from a semi-infinite medium" (1999), http://omlc.ogi.edu/news/may99/rd/index.html.
35. S. L. Jacques, "Reflectance spectroscopy with optical fiber devices and transcutaneous bilirubinometers," in *Biomedical Optical Instrumentation and Laser-Assisted Biotechnology*, A. M. Verga Scheggi, S. Martellucci, A. N. Chester, and R. Pratesi eds. (Kluwer Academic, Netherlands, 1996), pp. 83–94.
36. F. F. Jöbsis, "Noninvasive, infrared monitoring of cerebral and myocardial oxygen sufficiency and circulatory parameters," Science **198,** 1264–1267 (1977).
37. R. R. Anderson, and J. A. Parrish "The optics of human skin," J. Investig. Dermatol. **77,** 13–19 (1981).
38. S. T. Flock, S. L. Jacques, B. C. Wilson, W. M. Star, and M. J. C. van Gemert, "Optical properties of Intralipid: a phantom medium for light propagation studies," Lasers Surg. Med. **12,** 510–519 (1992).
39. H. J. van Staveren, C. J. M. Moes, J. van Marle, S. A. Prahl, and M. J. C. van Gemert, "Light scattering in Intralipid-10% in the wavelength range of 400–1100 nanometers," Appl. Opt. **30,** 4507–4514 (1991).

40. C. J. M. Moes, M. J. C. van Gemert, W. M. Star, J. P. A. Marijnissen, and S. A. Prahl, "Measurements and calculations of the energy fluence rate in a scattering and absorbing phantom at 633 nm," Appl. Opt. **28,** 2292–2296 (1989).
41. S. J. Madsen, M. S. Patterson, and B. C. Wilson, "The use of India ink as an optical absorber in tissue-simulating phantoms," Phys. Med. Biol. **37,** 985–993 (1992).
42. W. F. Cheong, S. A. Prahl, and A. J. Welch, "A review of the optical properties of biological tissues" (1996), http://omlc.ogi.edu/pubs/abs/cheong90a.html.
43. S. Fantini, M. A. Franceschini, J. B. Fishkin, B. Barbieri, and E. Gratton, "Quantitative determination of the absorption spectra of chromophores in strongly scattering media: a light-emitting-diode based technique," Appl. Opt. **33,** 5204–5213 (1994).
44. G. C. Holst, *CCD Arrays, Cameras, and Displays* (SPIE, Bellingham, Wash., 1996).
45. W. R. Blevin and W. J. Brown, "Effect of particle separation on the reflectance of semi-infinite diffusers," J. Opt. Soc. Am. **51,** 129–134 (1961).
46. M. J. C. van Gemert and W. M. Star, "Relations between the Kubelka-Munk and the transport equation models for anisotropic scattering," Lasers Life Sci. **1,** 287–298 (1987).
47. W. R. Blevin and W. J. Brown, "Light-scattering properties of pigment suspensions," J. Opt. Soc. Am. **51,** 975–982 (1961).
48. J. Reichman, "Determination of absorption and scattering coefficients for nonhomogeneous media 1: theory," Appl. Opt. **12,** 1811–1815 (1973).
49. J. B. Fishkin, O. Coquoz, E. R. Anderson, M. Brenner, and B. J. Tromberg, "Frequency-domain photon migration measurements of normal and malignant tissue optical properties in a human subject," Appl. Opt. **36,** 10–20 (1997).
50. D. Grosenick, H. Wabnitz, H. H. Rinneberg, K. T. Moesta, and P. M. Schlag, "Development of a time-domain optical mammograph and first *in vivo* applications," Appl. Opt. **38,** 2927–2943 (1999).
51. B. J. Tromberg, N. Shah, R. Lanning, A. Cerussi, J. Espinoza, T. Pham, L. Svaasand, and J. Butler, "Non-invasive *in vivo* characterization of breast tumors using photon migration spectroscopy," Neoplasia **2,** 26–40 (2000).
52. S. Fantini, S. A. Walker, M. A. Franceschini, M. Kaschke, P. M. Schlag, and K. T. Moesta, "Assessment of the size, position, and optical properties of breast tumors *in vivo* by non-invasive optical methods," Appl. Opt. **37,** 1982–1989 (1998).
53. T. J. Farrell, M. S. Patterson, and B. C. Wilson, "A diffusion theory model of spatially resolved, steady-state diffuse reflectance for the noninvasive determination of tissue optical properties *in vivo*," Med. Phys. **19,** 879–888 (1992).
54. P. Kubelka, "New contributions to the optics of intensely light-scattering materials. Part I," J. Opt. Soc. Am. **38,** 448–457 (1948).